

Natural Convection in a Square Cavity in the Presence of Heated Plate

P. Kandaswamy, J. Lee, A. K. Abdul Hakeem

School of Mechanical Engineering, Younsei University
Seoul, Republic of Korea

UGC-DRS Center for Fluid Dynamics, Department of Mathematics
Bharathiar University, Coimbatore 641 046, India
pgkswamy@yahoo.co.in

Received: 25.08.2006 **Revised:** 08.02.2006 **Published online:** 05.05.2007

Abstract. Natural convection heat transfer in a square cavity induced by heated plate is studied numerically. Top and bottom of the cavity are adiabatic, the two vertical walls of the cavity have constant temperature lower than the plate's temperature. The flow is assumed to be two-dimensional. The discretized equations were solved by finite difference method using Alternating Direction Implicit technique and Successive Over-Relaxation method. The study was performed for different values of Grashof number ranging from 10^3 to 10^5 for different aspect ratios and position of heated plate. Air was chosen as a working fluid ($Pr = 0.71$). The effect of the position and aspect ratio of heated plate on heat transfer and flow were addressed. With increase of Gr heat transfer rate increased in both vertical and horizontal position of the plate. When aspect ratio of heated thin plate is decreased the heat transfer also decreases. For the vertical situation of thin plate heat transfer becomes more enhanced than for horizontal situation.

Keywords: natural convection, heat transfer, heated plate.

Nomenclature

A	aspect ratio of the heated plate	\overline{Nu}	average Nusselt number
A_i	position of heated plates	p	pressure
g	acceleration due to gravity	t	dimensional time
Gr	Grashof number	T	dimensionless temperature
h_i	height of the heated plate	u, v	dimensional velocity components
H	height of the cavity	U, V	dimensionless velocity components
L	length of the cavity	x, y	dimensional coordinates
Nu	local Nusselt number	X, Y	dimensionless coordinates

Greek Symbols

α	thermal conductivity	Ψ	dimensionless stream function
β	volumetric co-efficient of thermal expansion	ρ	density
ν	kinematic viscosity	τ	dimensionless time
ω	dimensional vorticity	θ	dimensional temperature
ψ	dimensional stream function	ζ	dimensionless vorticity

Subscripts

c cold, h hot, $i = 1, 2$

1 Introduction

Over the past twenty years, a revolution in electronics has taken place. Natural convection cooling of components attached to printed circuit boards, which are placed vertically and horizontally in an enclosure is currently of great interest to the microelectronics industry. Natural convection cooling is desirable because it doesn't require energy source, such as a forced air fan and it is maintenance free and safe. Cavities with no obstructions in them have been studied in the past few decades(see [1–5]). The current interest has now shifted to complex cavities containing obstruction or partitions which has important implications in many branches of engineering particularly in microelectronics fabrication industry. Hence a number of convection studies both numerical and experimental are being conducted in this aspect.

Natural convection in an air filled, differentially heated, inclined square cavity with a diathermal partition placed at the middle of its cold wall was numerically studied for Rayleigh numbers 10^3 to 10^5 . It was observed that due to suppression of convection, heat transfer reductions upto 47 percent in comparison to the cavity without partition was observed by Frederick [6]. Laminar natural convection and conduction in enclosures with multiple vertical partitions are studied theoretically by Kangni et al. [7]. The study covers Rayleigh number Ra in the range 10^3 – 10^7 , $Pr = 0.72$ (air) aspect ratio 5–20, cavity width 0.1–0.9 and partition thickness 0.01–0.1. They found that the heat transfer decreases with increasing partition number (N) at high Rayleigh number for all conductivity ratios K_r and heat transfer decreases with increasing partition thickness C at all Ra except in the conduction regime where the effect is negligibly small. The off-center partitions are less effective in decreasing the heat transfer. Nusselt number is also a decreasing function in the aspect ratio A .

Shi and Khodadadi [8] have studied the effect of a thin fin on the hot wall of a differentially heated square cavity. The range of the Rayleigh number was 10^4 – 10^7 and length of fin equal to 20, 35 and 50 percent of the side. They reported that two competing mechanisms that are responsible for the flow and thermal modifications are identified. One is due to the blockage effect of the fin and the other one is extra heating of the fluid. The extra heating effect is promoted as the Ra increases. For high Ra the flow field is enhanced regardless of the fin's length and position. The symmetric and asymmetric variations of the Nusselt number on the hot wall were directly linked to the streamline

patterns and it formed thermal boundary layers above and below the fin. Heat transfer capacity on the hot wall was always degraded, on cold wall without fin can be promoted for high Ra and with the fin placed in the vicinity of the insulated walls. Tasnim and Collins [9] determined the effect of a horizontal baffle placed on hot (left) wall of a differentially heated square cavity. It has been found that adding baffle on the hot wall can increase the rate of heat transfer by as much as 31.46 percent compared with a wall without baffle for $Ra = 10^4$. When $Ra = 10^5$ the increase in heat transfer is 15.3 percent for the same baffle length and the increases in heat transfer is 19.73 percent, when the longest baffle is attached at the middle of the cavity.

The previous studies clearly indicate that the natural convection of baffle attached the vertical walls at different position and aspect ratio. The aim of the present work is to study natural convection in a cavity with a heated plate located at vertical and horizontal situation for different position and aspect ratio of the plate.

2 Mathematical analysis

Consider a two dimensional square cavity of height H and length L as shown in Fig. 1. The top and bottom walls of the cavity are adiabatic and the two vertical walls have constant temperature T_c lower than plate's temperature. The cartesian coordinates (x, y) with the corresponding velocity components (u, v) are as indicated in Fig. 1. The gravity g acts normal to the y direction. In this figure h is the length of plate, h_1 the distance of the plate to the parallel left wall for the first situation and the distance of the plate to the parallel upper wall for second situation, h_2 is the distance of center of plate to the perpendicular upper wall for first situation and to the perpendicular left wall for second situation.

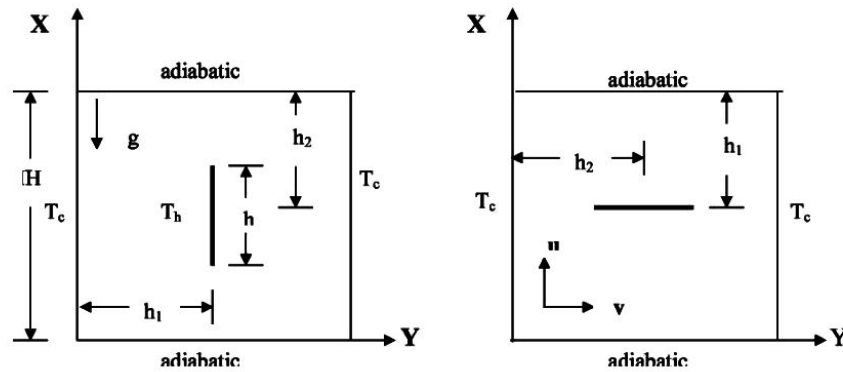


Fig. 1. Schematic diagram of the cavity: (a) vertical position of heated plate; (b) horizontal position of heated plate.

The non dimensional equations governing the laminar two-dimensional incompressible flow of the fluid under Boussinesq approximation in an environment described above

are

$$\frac{\partial \zeta}{\partial \tau} + U \frac{\partial \zeta}{\partial X} + V \frac{\partial \zeta}{\partial Y} = Gr \frac{\partial T}{\partial Y} + \nabla^2 \zeta, \quad (1)$$

$$\frac{\partial T}{\partial \tau} + U \frac{\partial T}{\partial X} + V \frac{\partial T}{\partial Y} = \frac{1}{Pr} \nabla^2 T, \quad (2)$$

$$\nabla^2 \psi = -\zeta, \quad (3)$$

where

$$U = -\frac{\partial \psi}{\partial Y}, \quad V = \frac{\partial \psi}{\partial X} \quad \text{with} \quad \zeta = \frac{\partial U}{\partial Y} - \frac{\partial V}{\partial X}.$$

The nondimensional parameters that appear in the equations are:

$$X = \frac{x}{L}, \quad Y = \frac{y}{L}, \quad U = \frac{u}{\nu/L}, \quad V = \frac{v}{\nu/L},$$

$$\tau = \frac{t}{L^2/\nu}, \quad T = \frac{\theta - \theta_c}{\theta_h - \theta_c}, \quad \psi = \frac{\psi}{\nu}, \quad \zeta = \frac{\omega}{\nu/L^2}$$

and the nondimensional parameters are: $Gr = \frac{g\beta(\theta_h - \theta_c)L^3}{\nu^2}$ – the Grashof number, $Pr = \frac{\nu}{\alpha}$ – the Prandtl number, $A = \frac{h}{H}$ – the aspect ratio of heated plate, $A_1 = \frac{h_1}{H}$ – position of the horizontal heated plate, $A_2 = \frac{h_2}{H}$ – position of the vertical heated plate.

The initial and boundary conditions in the dimensionless form are:

$$\tau = 0; \quad U = V = 0; \quad T = 0; \quad 0 \leq X \leq 1; \quad 0 \leq Y \leq 1,$$

$$\tau > 0; \quad U = V = 0; \quad \frac{\partial T}{\partial X} = 0; \quad \text{at } X = 0 \quad \text{and} \quad X = 1; \quad 0 \leq Y \leq 1,$$

$$U = V = 0; \quad T = 0; \quad \text{at } Y = 0 \quad \text{and} \quad Y = 1; \quad 0 \leq X \leq 1,$$

$$U = V = 0; \quad T = 1.$$

The local Nusselt number Nu is defined by

$$Nu = \frac{\partial T}{\partial Y} \Big|_{Y=0}$$

resulting in the average Nusselt number as

$$\overline{Nu} = \int_0^1 Nu dX.$$

3 The method of solution

The equations are solved numerically using finite difference method with a regular cartesian space grid. Suppose that all quantities $T_{i,j,n}$, $\zeta_{i,j,n}$, $\Psi_{i,j}^n$ are known at a time $n\Delta\tau$.

An alternating direction implicit (ADI) method is employed to find the temperature and vorticity values at the interior grid points in the next time level $(n + 1)\Delta\tau$. For this, forward difference approximation is used for time derivative and central difference approximations are used for all spatial derivatives. The method of successive over relaxation (SOR) is then used in conjunction with the newly computed temperatures $T_{i,j,n+1}$ and vorticities $\zeta_{i,j,n+1}$ to solve the stream function equation for the new improved stream function $\Psi_{i,j}^{n+1}$. After finding the stream function, the values of U and V at the current time level are computed using the central difference approximations to $U = -\frac{\partial\Psi}{\partial Y}$, and $V = \frac{\partial\Psi}{\partial X}$. This procedure is repeated at each time step. The boundary vorticities at the solid walls can be derived considering Taylor's series expansions for stream function in the vicinity of the walls. This computational cycle is repeated till steady state solution is obtained, that is, when the following convergence criteria

$$|\Phi_{i,j,n} - \Phi_{i,j,n+1}| < 10^{-5} \quad (4)$$

for temperature, vorticity and stream function is met. The results obtained by the code developed were validated against those of Zhong et al. [3] (see the Fig. 2(b)). We observe a good agreement. In order to determine the proper grid size for this study, a grid independence test was conducted for the Gr of 10^4 in a square cavity with a heated thin plate located at the middle of the cavity. The length of the thin plate was set to be half of the cavity length. Five different grid densities 21×21 , 31×31 , 41×41 , 51×51 and 61×61 . The minimum value of the stream function of the primary vortex (ψ_{min}) is commonly used as a sensitivity measure of the accuracy of the solution. Quantity (ψ_{min}) is selected as the monitoring variable for the grid independence study. Fig. 2(a) shows the dependence of quantity (ψ_{min}) on the grid size. Comparison of the predicated (ψ_{min}) values among five different cases suggests that the three grid distributions 41×41 , 51×51 and 61×61 gives nearly identical results. Considering both the accuracy and the computational time, the following calculations were all performed with a 51×51 grid system.

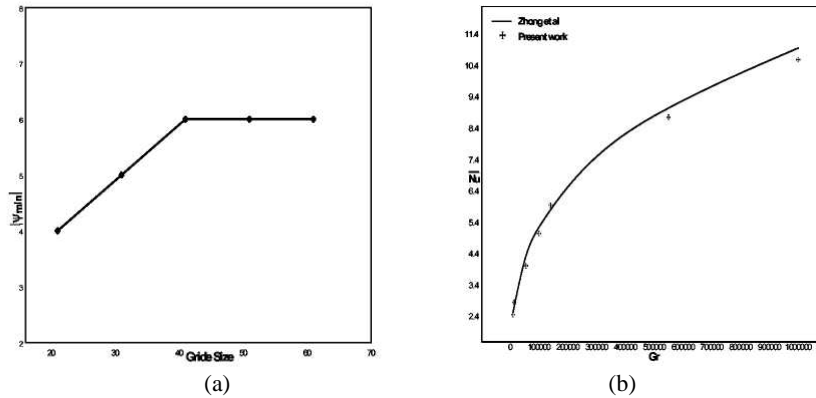


Fig. 2. (a) ψ_{min} as the function of the grid size; (b) correlation of present numerical results with others.

4 Results and discussions

Natural convection of low Prandtl number fluid (0.71), corresponding to air is investigated numerically, in the presence of a heated thin plate. The computations are carried out for a wide range of Grashof number Gr varying from 10^3 to 10^5 . The study was conducted for two different positions of the thin heated plate located at horizontal and vertical positions. The results are depicted as streamlines and isotherms plots. Hence the problem is symmetrical about center of the cavity. We have plotted both isotherms and streamlines in a single plot to study the effect of different locations of the horizontal plate. The rate of heat transfer across the cavity is calculated in terms of the average Nusselt number \overline{Nu} .

4.1 Thin plate located horizontally

When the heated thin plate is located horizontally the results are obtained by changing the aspect ratio and position of the plate. Fig. 3 show the streamlines and isotherms for $A = 0.5$ and plate is located at the center ($A_1 = 0.5$), for different values of Grashof numbers. When $Gr = 10^3$, fluid motion is symmetric in the cavity due to dominance of conduction mechanism. As Gr increases convection becomes stronger and rotation over the plate becomes stronger comparing to the one below the plate. When the aspect ratio of heated thin plate is increased the rotation of the fluid is very stronger. In addition as the space between the heated vertical boundary and plate is small, the rotation of fluid downward is prevented. The fluid flow below the plate produces stagnation point depending on the increase of Gr . Fig. 4 shows streamline and isotherms for $A = 0.2$



Fig. 3. Isotherms and streamlines for $A = 0.5$, $A_1 = 0.5$, $Gr = 10^3, 10^4$ and 10^5 .

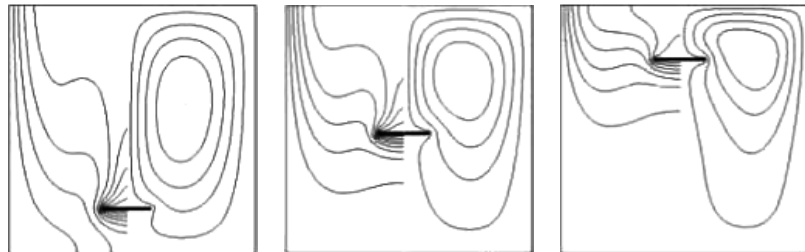


Fig. 4. Isotherms and streamlines for $Gr = 10^5$, $A = 0.2$, and $A_1 = 0.8, 0.5, 0.2$.

at $Gr = 10^5$ and different position of plate. The flow and temperature distribution in a cavity maintain the symmetrical behaviour. The recirculation spreads downward in the cavity because of the gap between vertical side walls and edges of the heated plate as seen in the figures. It is seen that the fluid flow under the plate does not change significantly. Fig. 5 shows the flow pattern for $A = 0.5$ and $Gr = 10^5$. For $A_1 = 0.8$, the resulting flow pattern is found to be bicellular and corresponding isotherm shows a weak convection type. When the position of plate is changed ($A_1 = 0.5$), the flow pattern remains same, but corresponding isotherm shows convection become strong and when $A_1 = 0.2$ then convection become very strong. The heat transfer is increased for increasing the aspect ratio of plate and convection mechanism is very effective as seen in Fig. 6. Another expected result is that if the hot plate is on the upper wall of the cavity there is no motion under the cavity.

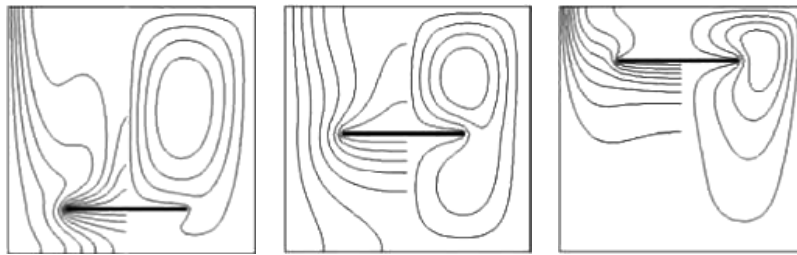


Fig. 5. Isotherms and streamlines for $Gr = 10^5$, $A = 0.5$, and $A_1 = 0.8, 0.5, 0.2$.

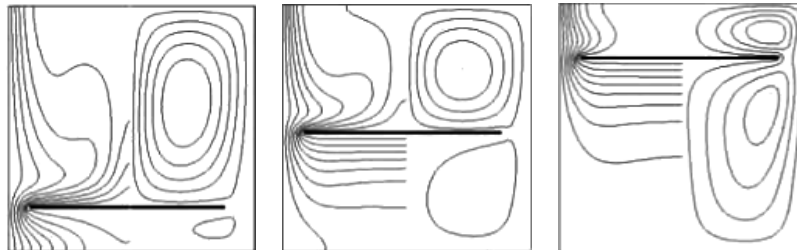


Fig. 6. Isotherms and streamlines for $Gr = 10^5$, $A = 0.8$, and $A_1 = 0.8, 0.5, 0.2$.

4.2 Thin plate located vertically

In this case, Fig. 7, 8 show the effect of Gr in a cavity when the plate is located vertically for aspect ratio $A = 0.5$ and $A_2 = 0.5$. For a $Gr = 10^3$, conduction mechanism is dominant. When increasing the Gr , the resulting flow pattern is found to be bicellular and corresponding isotherm shows a strong convection type as can be seen in the Fig. 7. When fixing $Gr = 10^5$ and plate is located at the center ($A_2 = 0.5$) then Fig. 8 shows the streamline and isotherm for different values of aspect ratio of heated plate. When heated plate aspect ratio is increased then convection mechanism is more effective than conduction and heat transfer also increases.

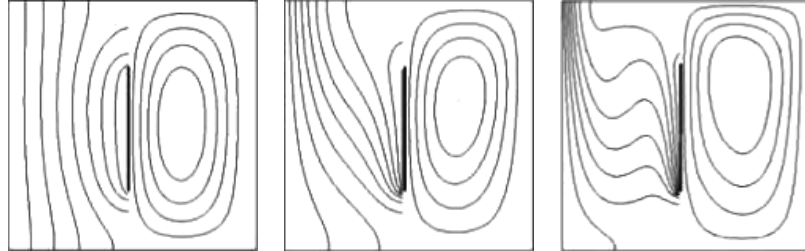


Fig. 7. Isotherms and streamlines for $A = 0.5$, $A_2 = 0.5$, $Gr = 10^3, 10^4$ and 10^5 .

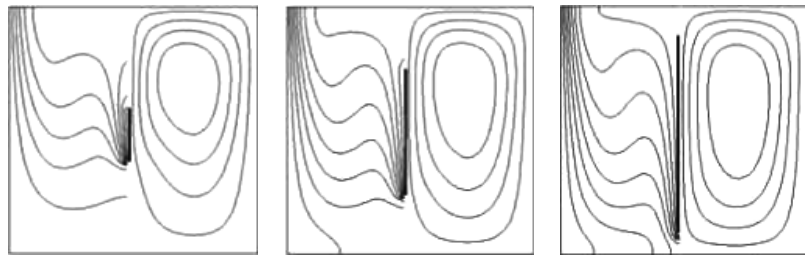


Fig. 8. Isotherms and streamlines for $Gr = 10^5$, $A_2 = 0.5$, and $A = 0.8, 0.5, 0.2$.

4.3 Over all heat transfer

The average Nusselt number serves as a measure of the heat transfer for two different position of the plate. In Fig. 9 Nusselt number is plotted for different Gr and different aspect ratio of heated thin plate for vertical situation. For a fixed aspect ratio of thin plate, when Grashof number is increased average Nusselt number also increases as seen in Fig. 9(b). In addition, for an increase in the aspect ratio of plate fixing Gr , the heat transfer also increases as seen in Fig. 9(a).

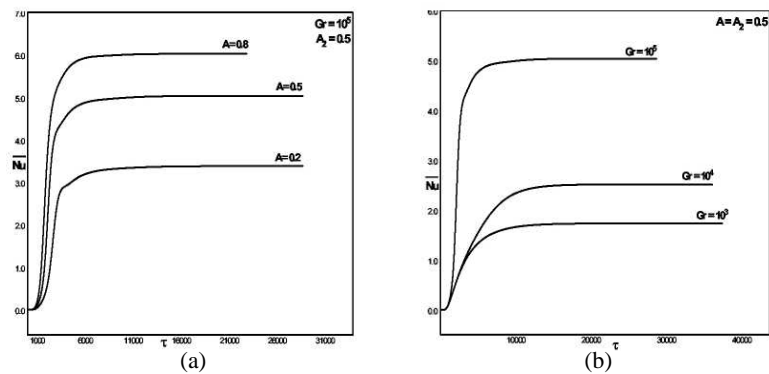


Fig. 9. (a) \overline{Nu} for vertical situation for different length of plate; (b) \overline{Nu} for vertical situation for different values of Gr .

Fig. 10 shows the heat transfer for different values of Gr and different values of aspect ratio of heated thin plate for horizontal situation. It was found that heat transfer rate increases for increase in Gr . The heat transfer rate increases when the aspect ratio of the plate increases.

When comparing the horizontal and vertical situation with each other it can be seen that overall heat transfer for higher Grashof number stays almost the same in both situations while heat transfer is higher for vertical situation than horizontal one for smaller Gr . It can be seen clearly in the Fig. 11 for $Gr = 10^5$. This means that in vertical situation heat transfer is more enhanced. In addition, flow motion in cavity depends on the position of thin plate.

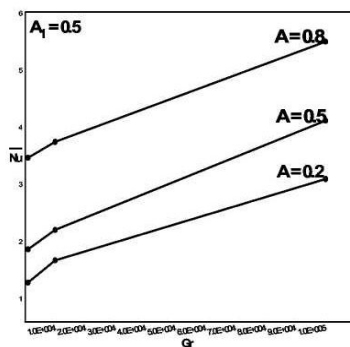


Fig. 10. \overline{Nu} for horizontal situation of plate.

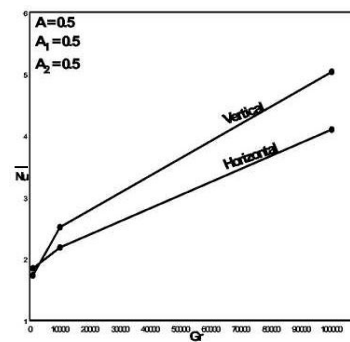


Fig. 11. \overline{Nu} for horizontal vertical situation of plate.

5 Conclusions

Buoyancy induced flow and heat transfer inside a square cavity due to a heated thin plate was investigated numerically for heated plate placed vertically/horizontally. The flow motion in cavity depends on the heated plate itself. For increase in Gr heat transfer increased in both vertical and horizontal situation. As the aspect ratio of heated thin plate is increased the heat transfer also increases. Heat transfers become more enhanced in vertical situation than in horizontal situation.

References

1. G. De Vahl Davis, Laminar natural convection in an enclosed rectangular cavity, *Int. J. Heat Mass Transfer*, **11**, pp. 1675–1693, 1968.
2. A. Bejan, *Convection Heat Transfer*, Wiley, New York, 1984.
3. Z. Y. Zhong, K. T. Yang, J. R. Lloyd, Variable property effects in laminar natural convection in a square enclosure, *ASME J. Heat Transfer*, **17**, pp. 133–138, 1985.
4. S. Ostrach, Natural convection in enclosure, *ASME J. Heat Transfer*, **110**, pp. 1175–1190, 1988.

5. S. Saravanan, P. Kandaswamy, Natural convection in low Prandtl number fluids with a vertical magnetic field, *ASME J. Heat Transfer*, **122**, pp. 602–606, 2000.
6. R. L. Frederick, Natural convection in an inclined square enclosure with a partition attached to its cold wall, *Int. J. Heat Mass Transfer*, **32**, pp. 87–94, 1989.
7. A. Kangni, R. Ben, E. Bilgen, Natural convection and conduction in enclosure with multiple vertical partitions, *Int. J. Heat Mass Transfer*, **34**, pp. 2819–2825, 1991.
8. X. Shi, J. M. Khodadadi, Laminar natural convection heat transfer in a differentially heated square due to a thin fin on the hot wall, *ASME J. Heat Transfer*, **125**, pp. 624–634, 2003.
9. S. T. Tansnim, M. R. Collins, Numerical analysis of heat transfer in a square cavity with a baffle on the hot wall, *Int. Com. Heat mass Transfer*, **31**, 639–650, 2004.